European Journal of Medicinal Chemistry 258 (2023) 115575

Contents lists available at ScienceDirect

European Journal of Medicinal Chemistry

journal homepage: www.elsevier.com/locate/ejmech

Research paper

New 4-(*N*-cinnamoylbutyl)aminoacridines as potential multi-stage antiplasmodial leads

Mélanie Fonte [a,*], Diana Fontinha [b], Diana Moita [b], Omar Caño-Prades [c], Yunuen Avalos-Padilla [c], Xavier Fernàndez-Busquets [c,d,e], Miguel Prudêncio [b], Paula Gomes [a,**], Cátia Teixeira [a,f]

[a] LAQV-REQUIMTE, Departamento de Química e Bioquímica, Faculdade de Ciências, Universidade do Porto, Portugal
[b] Instituto de Medicina Molecular, Faculdade de Medicina, Universidade de Lisboa, Portugal
[c] Nanomalaria Group, Institute for Bioengineering of Catalonia (IBEC), The Barcelona Institute of Science and Technology, Barcelona, Spain
[d] Barcelona Institute for Global Health (ISGlobal, Hospital Clínic-Universitat de Barcelona), Spain
[e] Nanoscience and Nanotechnology Institute (IN2UB), University of Barcelona, Spain
[f] Gyros Protein Technologies Inc., Tucson, AZ, USA

ARTICLE INFO

Handling Editor: Dr. Z Liu

Keywords:
Acridine
Antimalarial
Blood-stage
Cinnamic acid
Gametocyte
Hybrid
Liver-stage
Multi-target

ABSTRACT

A novel family of 4-aminoacridine derivatives was obtained by linking this heteroaromatic core to different *trans*-cinnamic acids. The 4-(*N*-cinnamoylbutyl)aminoacridines obtained exhibited *in vitro* activity in the low- or sub-micromolar range against (i) hepatic stages of *Plasmodium berghei*, (ii) erythrocytic forms of *Plasmodium falciparum*, and (iii) early and mature gametocytes of *Plasmodium falciparum*. The most active compound, having a *meta*-fluorocinnamoyl group linked to the acridine core, was 20- and 120-fold more potent, respectively, against the hepatic and gametocyte stages of *Plasmodium* infection than the reference drug, primaquine. Moreover, no cytotoxicity towards mammalian and red blood cells at the concentrations tested was observed for any of the compounds under investigation. These novel conjugates represent promising leads for the development of new multi-target antiplasmodials.

1. Introduction

Malaria is an infectious disease caused by protozoan parasites of the genus *Plasmodium* that remains a major concern in low-income tropical and sub-tropical countries. Despite the steady decrease in the malaria burden during the first decade of the 21st century, progress has stalled in the past five years. Moreover, global warming may favor the migration of the *Anopheles* mosquitoes, the disease's main vector, to currently malaria-free regions [1]. Among the reasons for malaria's ongoing burden are (i) the complex life cycle of the *Plasmodium* parasite, which hampers the swift and successful development of effective drugs and vaccines, and (ii) the fast selection and spread of drug-resistant parasite strains to all the drugs developed so far [2]. In fact, the world is now facing a concerning decline in the effectiveness of the frontline artemisinin-based combination therapies (ACT), as signs of resistance to this therapy has transposed the borders of Southeast Asia and has spread even to Africa [3–7]. This highlights the pressing need to discover new potent and safe antimalarial drugs, ideally, cost-effective since malaria mostly affects low-income populations, and actives against multiple stages of the life cycle of different *Plasmodium* species to decrease the probability of resistance appearance [8].

One cost-effective strategy towards affordable medicines is based on rescuing old antimalarial pharmacophores, through chemical modifications, aiming at their re-introduction in the antimalarial chemotherapy arsenal [9,10]. In this regard, our research group have been working on the rescuing of classical antimalarial drugs like quinacrine (QN), chloroquine (CQ), and primaquine (PQ), which their use has been limited due to toxicity and resistance issues [11–18]. QN, an acridine-based compound, was the first synthetic antimalarial drug and its potent blood-schizonticidal activity turned it into a promising substitute for quinine, the first effective therapy used against malaria [10,19]. However, the serious side effects of QN led to its rapid replacement

* Corresponding author.
** Corresponding author.
E-mail addresses: up201305020@edu.fc.up.pt (M. Fonte), pgomes@fc.up.pt (P. Gomes).

https://doi.org/10.1016/j.ejmech.2023.115575
Received 14 April 2023; Received in revised form 9 June 2023; Accepted 14 June 2023
Available online 22 June 2023

by CQ, which displayed higher efficiency, oral bioavailability and safety. Still, the use of CQ to treat malaria has been gradually abandoned due to the emergence and spread of CQ-resistant strains of *P. falciparum*, the most lethal agent of human malaria [19,20]. While most antimalarial agents available, such as the case of QN and CQ, target blood-stage parasites, PQ remained, for many years, the only drug in clinical use that (i) acts against liver forms of all *Plasmodium* species, including the latent hypnozoites of *P. vivax* and *P. ovale* that can cause malaria relapses, and (ii) efficiently eliminates gametocytes, the mosquito vector-infective forms of malaria parasites [21]. Nevertheless, PQ also presents significant downsides that limit its clinical application, including its high hemotoxicity and low oral bioavailability [22,23]. Recently, in 2018, the Food and Drug Administration approved tafenoquine (TQ), which has higher efficacy due to its superior pharmacokinetic properties, but is also hemotoxic and, like PQ, cannot be used in G6PD-unknown or -deficient patients [24]. Thus, our latest efforts focused on the development of novel QN analogues merging both the CQ and the PQ cores in a single structure (**1a-c**, Fig. 1), as potential multi-stage antiplasmodials [17,18]. Multi-target drugs have raised considerable interest in the last decade owing to their advantages in the treatment of complex diseases such as malaria and drug resistance issues [25,26]. 4-*N*-butylaminoacridine (**1a**), the best derivative from this family, displayed promising results since the compounds retained the activity of the parent drugs, CQ and PQ, showing significant *in vitro* activity against both liver and blood stages malaria parasites. Based on this and inspired by the "covalent bitherapy" concept first advanced by Meunier [27,28], which advocates the combination of two pharmacophores in one molecule, our working hypothesis was that conjugation of 4-*N*-butylaminoacridine (**1a**) to bioactive *trans*-cinnamic acids would afford new constructs (**2a-l**) with improved efficacy and safety in multiple stages of malaria parasite life cycle while being less likely to elicit resistance. This "covalent bitherapy" approach has already been successfully employed in the preparation of compounds with pronounced antimalarial activity [29,30]. Cinnamic acid derivatives, due to their α,β-unsaturated carbonyl moiety, can act as Michael acceptors and inhibit cysteine proteases, especially falcipain-2 and falcipain-3, involved in hemoglobin degradation and thus vital for the intra-erythrocytic stage of the parasite [31–36]. In this sense, we choose *trans*-cinnamic acids not only to introduce the α,β-vinylcarbonyl moiety (Michael acceptor), but also because of their antimalarial potential that was advanced by Kanaani and Ginsburg in 1992, based on cinnamic acids' ability to inhibit lactate transport, the major product of parasite energy metabolism and, thus, vital for the survival and growth of intraerythrocytic parasites. These authors also confirmed that cinnamic acid derivatives hampered the production of ATP by the parasite and inhibited the transport of glucose, glycine, and sorbitol by *Plasmodium*-infected erythrocytes [37,38]. Since then, conjugation of cinnamic acids with classical antimalarials such as CQ, QN and PQ has been studied by different groups [39,40], including ours [15,16,41,42], and has delivering promising *in vitro* antiplasmodial results [39,43]. In view of this, we have coupled a series of twelve different *trans*-cinnamoyl moieties to the aliphatic amino group of **1a**, and evaluated their *in vitro* activity against the liver, blood and gametocyte stages of *Plasmodium* parasites, aiming at the establishment of relevant structure-activity relationship (SAR). The data herein obtained demonstrated that the new conjugates preserved and, in some cases, improved multi-stage activity *in vitro* and that this activity is very dependent of the *trans*-cinnamoyl moiety coupled to the aliphatic amino group of **1a**.

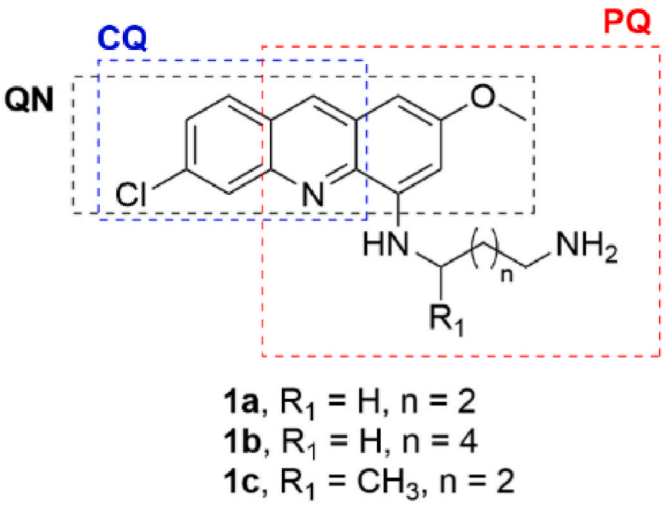

Fig. 1. QN analogues with dual-stage antiplasmodial activity previously reported by Fonte *et al.* [18].

2. Results and discussion

2.1. Chemistry

The chemical synthesis of target compounds **2a-l** was carried out *via* the synthetic route presented in Scheme 1. Detailed procedures and relevant spectroscopic data of the final compounds are provided in Section 4 and in Supplementary Information (SI).

The QN analogue 4-(4-aminobutyl)amino-6-chloro-2-methoxy-acridine (**1a**) was first obtained by a ten-step synthetic route starting from the commercial compound 4-chlorosalicylic acid, as previously reported [17,18]. Compound **1a** was then coupled to a series of *trans*-cinnamic acids by a standard *in situ* amide coupling method, using O-(Benzotriazol-1-yl)-*N,N,N′,N′*-tetramethyluronium tetrafluoroborate (TBTU) and *N,N*-diisopropylethylamine (DIEA) as a coupling agent and base, respectively, to afford the target compounds **2a-l**. To this end, the carboxylic acid group in the *trans*-cinnamic acid was first activated for 1 h with TBTU and DIEA, in dichloromethane (DCM); after the activation period, **1a** was added to the mixture and the reaction allowed to proceed at room temperature (r.t.). The crude products were purified by liquid chromatography on silica-gel columns, to obtain the target compounds in 95–99% purity, as confirmed by high-performance liquid chromatography (HPLC). Structural analyses by electrospray ionization-ion trap mass spectrometry (ESI-IT MS), and by proton (^{1}H) and carbon-13 (^{13}C) nuclear magnetic resonance (NMR) confirmed the expected structures for all target compounds **2a-l**, which were obtained in moderate to excellent overall yields (33–95%).

2.2. Biological assays

2.2.1. Hepatic stage activity

The *in vitro* activity previously observed for QN analogue **1a** against hepatic forms of *P. berghei* parasites revealed the importance of including the aminoalkyl side chain in position 4 of the acridine ring, since, according to the literature, QN has poor activity against liver stage parasites and a low selectivity index [16]; moreover, such modification did not abolish the blood stage activity typical of QN and related compounds [18]. Advancing drug candidates that eliminate liver stage parasites is highly relevant, as they are not only scarce [22], but may also hamper the development of thousands of erythrocyte-infective merozoites responsible for disease symptoms [44,45]. Therefore, based on our previous studies showing that *N*-cinnamoylation of the classical antimalarial drugs CQ, PQ and QN led to an improvement of liver stage activity, we hypothesized that a similar benefit might result from coupling **1a** to *trans*-cinnamic acids to produce conjugates **2a-l**. Hence, *in vitro* activity of 1 and 10 μM **2a-l** against the hepatic stage of *P. berghei* infection was evaluated using a previously described bioluminescence-based method to quantify the parasite load of human hepatoma (Huh-7) cells [18]. The toxicity of the compounds to this human cell line was also assessed through the fluorescence measurement of cell confluency (Fig. 2), as described in detail in Section 4. Our

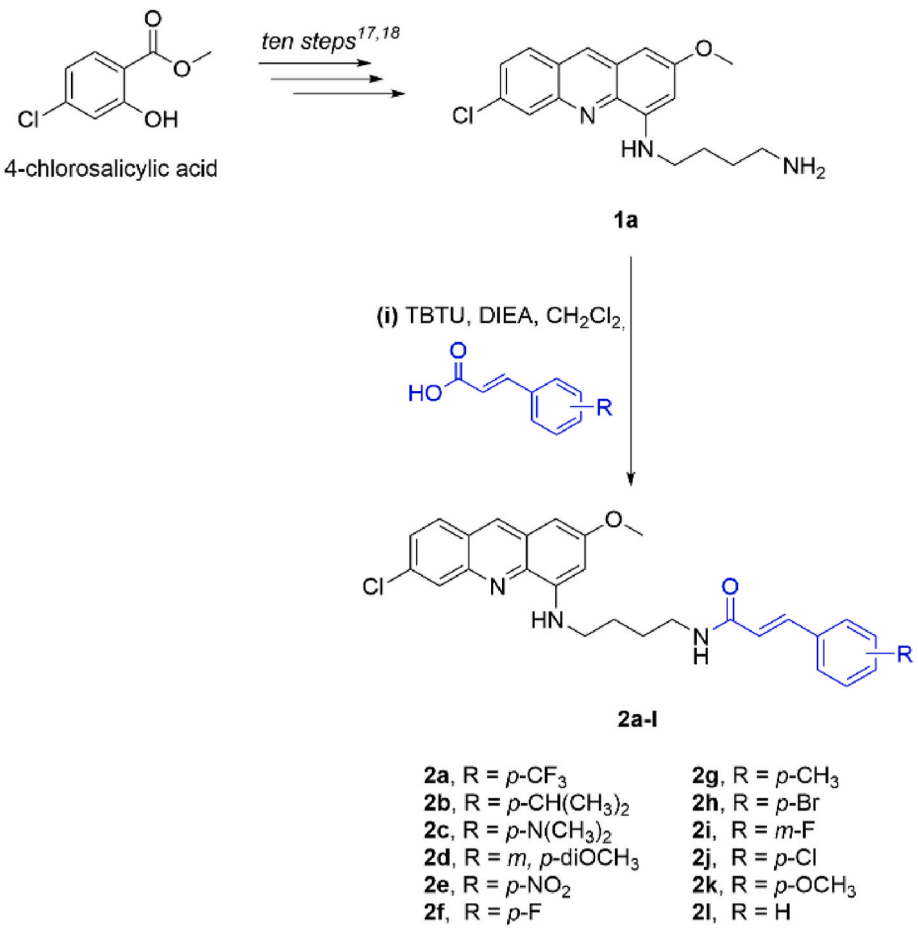

Scheme 1. Synthetic route to target compounds **2a-l**[a]
[a]The QN analogue **1a** was first obtained in ten steps as previously described [17,18], and subsequently coupled to different *trans*-cinnamic acids (highlighted in blue) under the following conditions: respective *trans*-cinnamic acid (1.1 equiv), TBTU (1.1 equiv), DIEA (2 equiv) and DCM at r.t.

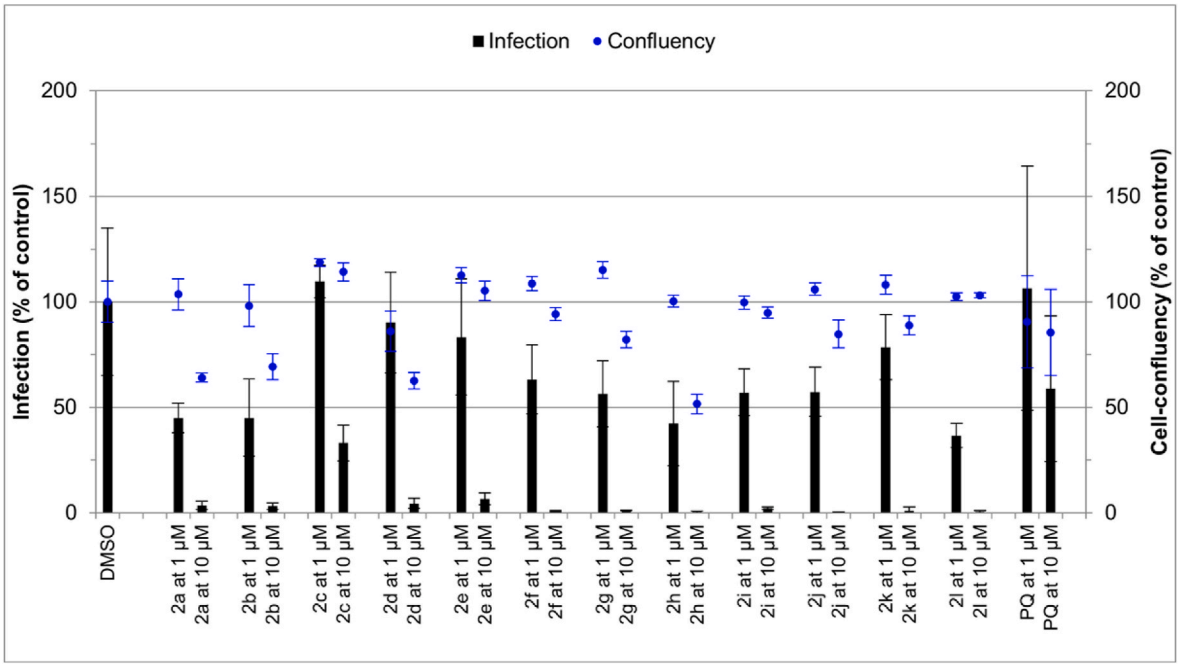

Fig. 2. *In vitro* activity of compounds **2a-l** and PQ, at 1 and 10 µM, against liver forms of *P. berghei*. Cytotoxicity to Huh7 cells (cell confluency scale, blue circles) are also shown.

results show that all the compounds **2a-l** were more active than the reference drug PQ against hepatic forms of *P. berghei* (Fig. 2).

IC_{50} values were then determined for the most active and least cytotoxic (above ~75% confluency relative to control) compounds at the highest concentration tested, 10 μM (**2e-f, i-l**). All IC_{50} values obtained were in the low- or sub-micromolar range ($0.496 < IC_{50} < 1.189$ μM) (Table 1). All *N*-cinnamoyl conjugates **2a-l** were more active than their parent compound **1a** ($IC_{50} = 2.22$ μM), which is in support of our initial hypothesis. The IC_{50} values were dependent on the substituent of the aryl ring in the cinnamoyl building block (R), and the following observations can be made in this regard.

(i) adding a substituent to the aryl ring of the cinnamoyl moiety seems to be slightly deleterious for liver stage activity, as compound **2l** (R═H) was the most active of the set ($IC_{50} = 0.496$ μM);
(ii) amongst the aryl substituents (i.e., R ≠ H, **2a-k**), the halogens led to higher activities, which seemed to increase with the size of the halogen atom, i.e., follow the order **2f** (R = *p*-F; $IC_{50} = 0.884$ μM) > **2j** (R = *p*-Cl; $IC_{50} = 0.998$ μM) > **2h** (R = *p*-Br); however, the *p*-bromine-substituted compound, **2h**, was significantly toxic to Huh-7 cells, hence its IC_{50} against hepatic stage parasites could not be reliably determined;
(iii) changing the position of the aryl substituent from *para* to *meta*, as in **2f** (R = *p*-F; $IC_{50} = 0.884$ μM) *versus* **2i** (R = *m*-F; $IC_{50} = 0.561$ μM), increased slightly the *in vitro* activity;
(iv) compared to all the previously mentioned ones, and regardless of their electron-withdrawing or -donating nature, polyatomic R groups, as in **2a** (R = *p*-CF_3), **2b** (R = *p*-$CH(CH_3)_2$; 0.129 μM), **2c** (R = *p*-$N(CH_3)_2$), **2e** (R = *p*-NO_2; $IC_{50} = 1.189$ μM), or **2k** (R = *p*-OMe; 1.182 μM), were not advantageous, as they led to either a decrease in liver stage activity (**2c,e,k**) or a clear increase in cytotoxicity at 10 μM (**2a,b**); insertion of a second substituent, as in **2d** (R = *o*,*m*-di(OMe)) further aggravated the latter.

Overall, conjugates **2i** and **2l** stood out for their higher activity against hepatic forms of *P. berghei*, being approximately 25-fold more potent than the reference drug PQ, while not showing any significant toxicity to Huh-7 cells up to 10 μM.

2.2.2. Gametocytocidal activity

Like antiplasmodials targeting liver stage *Plasmodium* parasites, those that are able to kill gametocytes are also highly important, but scarce. Since gametocytes are the only forms of *Plasmodium* that are infective to the mosquito vector, their elimination hampers the host-to-vector transmission, therefore blocking the dissemination of the disease. As such, the gametocytocidal activity of compounds **2a-l** was also assessed *in vitro* against early gametocytes of *P. falciparum* (3D7 strain) using the test compounds at 5 μM, which is the IC_{10} value for the reference drug PQ. Results depicted in Fig. 3 are expressed as % of inhibition of gametocyte growth and show that the inhibitory activity of conjugates **2a-l** is comparable to (**2a, 2c, 2d, 2f, 2h** and **2j**, 15–30%

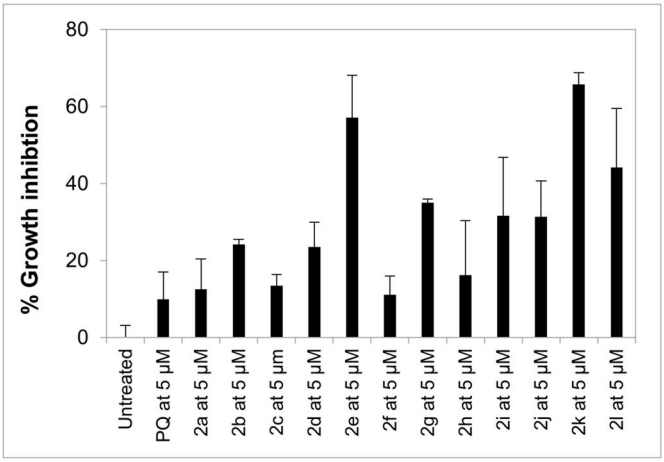

Fig. 3. *In vitro* growth inhibition of early *P. falciparum* 3D7 gametocytes upon incubation with test compounds **2a-l** at 5 μM; PQ was included as the reference gametocytocidal drug.

Table 1
In vitro activity of compounds **2a-l** against liver forms of *P. berghei*, as well as early gametocytes and ring stages of *P. falciparum* 3D7.

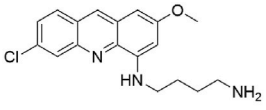

1a

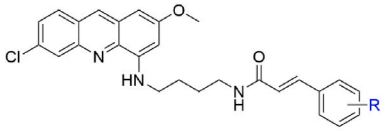

2a-l

Compound	R	Liver stage[a] (IC_{50} ± SD, μM)	Gametocyte stage[b] (IC_{50} ± SD, μM)	Blood stage[c] (IC_{50} ± SD, μM)
1a	–	2.22 ± 0.51[d]	–	5.64 ± 0.22[d]
2a	*p*-CF_3	ND[b]	–	–
2b	*p*-$CH(CH_3)_2$	0.129 ± 0.063	–	–
2c	*p*-$N(CH_3)_2$	–	–	–
2d	*m, p*-diOCH_3	–	–	–
2e	*p*-NO_2	1.189 ± 0.163	16.33 ± 1.29	3.82
2f	*p*-F	0.884 ± 0.046	–	5.83
2g	*p*-CH_3	ND[e]	0.63 ± 0.35	10.82
2h	*p*-Br	ND[e]	–	–
2i	*m*-F	0.561 ± 0.179	0.14 ± 0.43	4.34
2j	*p*-Cl	0.998 ± 0.103	–	–
2k	*p*-OCH_3	1.182 ± 0.115	0.52 ± 0.38	10.30
2l	H	0.496 ± 0.230	6.66 ± 1.54	>70
PQ	–	12.255 ± 2.001	17.66 ± 2.31	–
CQ	–	–	–	0.02[d]

[a] Liver-stage antiplasmodial activity was determined against *P. berghei*, using PQ as reference drug.
[b] Gametocytocidal activity was determined in *P. falciparum* NF54-gexp02-Tom strain, using PQ as reference drug.
[c] Blood-stage antiplasmodial activity was determined against the CQ-sensitive *P. falciparum* 3D7 strain, using CQ as reference drug.
[d] Value taken from Ref. [18].
[e] Not determined due to its high toxicity to Huh-7 cells.

inhibition) or higher than (**2e, 2g, 2i, 2k** and **2l**, >40% inhibition) that of PQ. IC_{50} values were determined for the top-five compounds (Table 1), which revealed that 2e (IC_{50} = 16.33 μM) was comparable to PQ (IC_{50} = 17.66 μM), while the remaining four compounds displayed stronger gametocytocidal activity (6.66 > IC_{50} > 0.14 μM) than the reference drug. The influence of substituent R on the gametocytocidal activity of conjugates **2a-l** was perceptible, but clear SAR could not be drawn, as the three best compounds, 2g (R = *p*-CH_3; IC_{50} = 0.63 μM), 2i (R = *m*-F; 0.14 μM) and 2k (R = *p*-OCH_3; IC_{50} = 0.52 μM) have R groups with quite distinct stereo-electronic properties and even occupy different positions in the aryl ring.

2.2.3. Blood stage activity

Motivated by the encouraging results obtained for the activity of the compounds against both liver and gametocyte stages of *Plasmodium* parasites, we further tested the blood stage activity of **2e, 2g, 2i, 2k** and **2l**, i.e., the top-five gametocytocidals, which includes the top-two compounds against liver forms of the parasite. The *P. falciparum* 3D7 strain was used to assess the effect of the compounds *in vitro* against blood stage parasites by means of flow cytometry, employing the SYTO 11 green-fluorescent nucleic acid stain. The hemolytic activity of the compounds at 20 μM was assessed in parallel, and none was found significantly hemolytic at this concentration. As for blood antiplasmodial activity (Table 1), except for the unsubstituted (R═H) derivative **2l** (IC_{50} > 70 μM), all other compounds displayed IC_{50} values in the low micromolar range. Still, none of them could match the potent activity of the reference drug CQ against the same *P. falciparum* 3D7 strain (IC_{50} = 0.02). As described for the gametocytocidal activity, no clear SAR could be drawn in regard to blood stage activity because the set of compounds tested was not large enough to allow withdrawing any meaningful conclusions. Nevertheless, it appears that electron-withdrawing R groups, such as *p*-NO_2 in **2e** (IC_{50} = 3.82 μM), *p*-F in **2f** (IC_{50} = 5.827 μM) and *m*-F in **2i** (IC_{50} = 4.34 μM), lead to higher activity than electro-donating ones, as in **2g** (R = *p*-CH_3; IC_{50} = 10.82 μM) and **2k** (R = *p*-OCH_3; IC_{50} = 10.3 μM).

The data compiled in Table 1 proves the validity of our working hypothesis, since the second-generation compounds (**2a-l**) herein reported display the expected multi-stage activity *in vitro* of with no increase in cytotoxicity, as compared to the parent compound **1a**. Actually, the new compounds are more active against liver and gametocyte stages of parasite development than the reference drug, PQ, and more active than the parent drug **1a** against the erythrocytic stage. Therefore, the moiety newly introduced clearly has a positive impact on overall antiplasmodial activity. Ongoing studies *in vitro* (undisclosed data) will allow us to check whether falcipain inhibition may play a role in the slight increase in blood-stage activity of the 2nd generation compounds reported.

The exact mechanism of QN's antimalarial action remains unclear, but it has been demonstrated that QN can interact with β-hematin, consequently inhibiting hemozoin formation and the development of intraerythrocytic parasites. However, other mechanisms of action have been suggested to elucidate the antimalarial activity of QN derivatives, such as (i) inhibition of: the parasite's NF-κB pathway, the mitochondrial bc1 complex, and/or the parasitic DNA topoisomerases II; (ii) activation of the p53 pathway; and/or (iii) binding to DNA, either by intercalation or by groove binding [46,47]. On the other hand, as mentioned above, cinnamic acids are reported as inhibitors of lactate, glucose, glycine, and sorbitol transport by *Plasmodium*-infected erythrocytes and as being able to hinder the production of ATP by the parasite [37]. Therefore, both QN and cinnamic acid derivatives are reported to affect crucial pathways in the growth and survival of *Plasmodium*-infected erythrocytes. Yet, the new compounds herein reported are new molecular entities that may owe their multi-stage antiplasmodial action by effects other than those described to their separate building blocks, or by a combination of (a few) of them. Previous studies in our group focused on similar chloroquine-cinnamic acid conjugates demonstrated their ability to strongly interact with DNA [48], and preliminary studies (undisclosed data) on the compounds now reported point to a similar direction. Further studies will be conducted to deliver conclusive data on mode of action and possible off-target effect. Still, the lack of significant toxicity of the new compounds to either hepatocytes or erythrocytes are suggestive of a selective action.

3. Concluding remarks

Herein, we report the synthesis and *in vitro* evaluation of a new family of compounds **2a-l**, as promising multi-stage antiplasmodial leads obtained through the coupling of a series of *trans*-cinnamic acids to the aliphatic amine of the 4-aminoacridine **1a**, which we previously found to present dual-stage antiplasmodial activity *in vitro* [18]. Our working hypothesis was that the antimalarial activity of **1a** might be improved via such *N*-cinnamoylation procedure, in light of our earlier findings showing that a similar modification was applied to the classical antimalarial drugs PQ, CQ and QN [15,16,41,42]. This hypothesis was confirmed by the data obtained, as they demonstrate that the new conjugates preserve multi-stage activity *in vitro*, being more active against liver and gametocyte stages of parasite development than the reference drug, PQ. In fact, one compound (**2i**) showed a 20- and 120-fold higher activity than PQ against liver and gametocyte stages, respectively, alongside low micromolar activity against blood stage *P. falciparum* parasites. Blood-stage activity of the new compounds is not spectacular; still, some of them represent an improvement over the first-generation compound **1a**, while preserving relevant activity against other stages of parasite development. This provides confirmation of our working hypothesis and, together with results from ongoing mechanistic studies, offers an important advance towards the fine tuning of this type of molecular scaffolds envisaging their improvement as multi-stage antiplasmodial leads. These findings are in line with previous reports by other authors on the beneficial role not only of conjugation to *trans*-cinnamic acids, but also of fluorination in antimalarial drug discovery [49]. Moreover, none of the new compounds reported herein showed significant toxicity to either hepatic Huh-7 cells or erythrocytes. The fact that no compound at 20 μM was found to be significantly hemolytic is very important since the main problem associated to drugs active in liver stages, as PQ, is the hemolytic toxicity in G6PD-unknown or -deficient patients.

Altogether, these are encouraging results highlight scaffolds like **2i** as novel potential multi-stage antiplasmodial leads. Considering the importance of halting progression of infection at its very onset in the host, i.e., during the liver stage of the parasite's life cycle, and of avoiding its vector-mediated dissemination from infected to healthy people, these findings are a promising starting point that may have a relevant impact in the future development of antimalarial candidates.

4. Experimental Section

4.1. Chemistry

4.1.1. Chemicals and instrumentation

The chemicals and solvents used in this study were purchased from Sigma-Aldrich (*trans*-4-(trifluoromethyl)cinnamic acid, *trans*-4-nitrocinnamic acid, *trans*-3-fluorocinnamic acid and *trans*-4-(dimethylamino) cinnamic acid), Bachem (TBTU), Alfa Aesar (DIEA, *trans*-4-isopropylcinnamic acid), Acros organics (*trans*-cinnamic acid, *trans*-4-chlorocinnamic acid, *trans*-4-methoxycinnamic acid and *trans*-4-methylcinnamic acid), PanReac AppliChem (anhydrous Na_2SO_4), Biochem Chemopharma ($NaHCO_3$), VWR international (HPLC gradient grade, LC-MS grade and p.a. grade solvents, i.e., acetonitrile and methanol), LabChem (synthesis grade solvents, i.e., DMF, DCM, hexane and ethyl acetate), and CortecNet (deuterated solvents for NMR analysis). Aluminium foils coated with silica-gel 60 F254 from Merck were used for monitoring reaction progress, purification steps, and determination

of compound retention factors (R_f) by thin-layer chromatography (TLC). TLC chromatograms were revealed with ultra-violet light (254 nm), using a Viber Lourmat lamp, model CN-6. The purifications of compounds were performed by normal phase liquid chromatography using silica gel 60 from Sigma-Aldrich as solid-phase and a mixture of hexane and ethyl acetate 1:1 (v/v) as mobile-phase. ESI-IT MS analyses (positive mode) were achieved with solutions of the pure products in methanol, using a Finnigan Surveyor LCQ DECA XP MAX spectrometer, at the Department of Chemistry and Biochemistry of the Faculty of Sciences of the University of Porto. ^{1}H NMR and ^{13}C NMR spectra were recorded on a Bruker Avance III spectrometer at frequencies of 400 mHz and 100 mHz, respectively, and samples were prepared in hexadeuterated dimethylsulfoxide (DMSO-d_6) and deuterated chloroform ($CDCl_3$) with tetramethylsilane (TMS) as an internal reference. The determination of the retention times (RT) and purity degrees of compounds n was carried out by analytical HPLC, using a Hitachi-Merck Elite LaChrom system equipped with an L-2130 quaternary pump, an L-2200 thermostatted (Peltier effect) automated sampler, and an L-2455 diode-array detector (DAD). The compounds were dissolved in acetonitrile and injected in a reverse phase column (C18) Purospher star RP-C18 of 125 × 4.0 mm and 5 μm pore size. A gradient elution from 1 to 100% of acetonitrile in 0.05% aqueous (aq.) trifluoroacetic acid (TFA) was carried out for 30 min, at a flow rate of 1 mL min^{-1}, and detection was set at 220 nm.

4.1.2. General procedures. Compound 1a

The 4-(4-aminobutyl)amino-6-chloro-2-methoxy-acridine **(1a)** was prepared by a 10-step route previously described by us, and its structural data agreed with those earlier reported [18]. **Compounds 2a-l.** TBTU (1.1 equiv) and DIEA (2 equiv) were added to a solution of the *trans*-cinnamic acid of interest (1 equiv) in DCM. After 1 h of activation, a solution of 1a (1 equiv) in DCM was added to the mixture, and the reaction allowed to proceed at r.t. until no further progress could be observed by TLC (1–3 h). The mixture was then washed with saturated aq. $NaHCO_3$ (3 x 50 mL) and saturated aq. NaCl (3 x 50 mL), and the organic layer was collected and dried over anhydrous Na_2SO_4. The resulting suspension was filtered by gravity, and the filtrate evaporated to dryness under reduced pressure. The crude product thus obtained was purified by column chromatography on silica gel using hexane/ethyl acetate 1:1 (v/v) as eluent to afford compounds **2a-l** with purity degrees between 94.8 and 99.8% (HPLC) and correct structural data (NMR and ESI-IT-MS), as given in detail below. Chromatographic and spectral traces are provided in the SI.

4.1.2.1. (E)-N-(4-((6-chloro-2-methoxyacridin-4-yl)amino)butyl)-3-(4-(trifluoromethyl)phenyl)acrylamide (2a). Yellow solid, η = 67%; ^{1}H NMR (400 MHz, DMSO-d_6) δ 8.75 (s, 1H), 8.26 (t, J = 5.7 Hz, 1H), 8.13 (d, J = 2.1 Hz, 1H), 8.09 (d, J = 9.0 Hz, 1H), 7.76 (s, 4H), 7.55 (dd, J = 8.9, 2.1 Hz, 1H), 7.49 (d, J = 15.8 Hz, 1H), 6.76 (d, J = 15.9 Hz, 1H), 6.71–6.74 (m, 1H), 6.61 (d, J = 2.5 Hz, 1H), 6.30 (d, J = 2.5 Hz, 1H), 3.87 (s, 3H), 3.35–3.37 (m, 2H), 3.26–3.31 (m, 2H), 1.72–1.80 (m, 2H), 1.60–1.67 (m, 2H); ^{13}C NMR (100 MHz, DMSO-d_6) δ 164.88, 159.58, 145.33, 144.59, 139.55, 138.82, 137.27, 133.79, 133.33, 130.18, 128.57, 128.44, 127.67, 127.13, 126.26, 126.23, 126.00, 125.62, 97.01, 90.66, 55.60, 42.64, 39.01, 27.35, 26.26; $^m/_z$ (ESI-IT MS, +) 528.47 (M + H$^+$); M$^+$ ($C_{28}H_{25}ClF_3N_3O_2$) requires 527.16; HPLC-DAD: RT, 28.2 min; purity degree (peak relative area), 99.7%.

4.1.2.2. (E)-N-(4-((6-chloro-2-methoxyacridin-4-yl)amino)butyl)-3-(4-isopropylphenyl)acrylamide (2b). Orange solid, η = 63%; ^{1}H NMR (400 MHz, DMSO-d_6) δ 8.75 (s, 1H), 8.16–8.08 (m, 3H), 7.56 (dd, J = 9.0, 2.1 Hz, 1H), 7.49–7.44 (m, 2H), 7.38 (d, J = 15.8 Hz, 1H), 7.30–7.25 (m, 2H), 6.72 (t, J = 5.8 Hz, 1H), 6.61 (d, J = 2.4 Hz, 1H), 6.57 (d, J = 15.8 Hz, 1H), 6.30 (d, J = 2.5 Hz, 1H), 3.87 (s, 3H), 3.41–3.34 (m, 2H), 3.26 (q, J = 6.6 Hz, 2H), 1.82–1.71 (m, 2H), 1.69–1.56 (m, 2H); ^{13}C NMR (100 MHz, DMSO-d_6) δ 164.99, 159.09, 149.88, 144.84, 144.10, 138.34, 133.29, 132.83, 132.61, 129.68, 127.94, 127.51, 127.19, 126.83, 126.64, 125.51, 121.36, 96.51, 90.17, 55.10, 42.17, 38.44, 33.26, 26.94, 25.79, 23.65; $^m/_z$ (ESI-IT MS, +) 502.52 (M + H$^+$); M$^+$ ($C_{30}H_{32}ClN_3O_2$) requires 501.22; HPLC-DAD: RT, 29.3 min; purity degree (peak relative area), 99.5%.

4.1.2.3. (E)-N-(4-((6-chloro-2-methoxyacridin-4-yl)amino)butyl)-3-(4-(dimethylamino)phenyl)acrylamide (2c). Orange solid, η = 71%; ^{1}H NMR (400 MHz, DMSO-d_6) δ 8.75 (s, 1H), 8.15–8.13 (m, 1H), 8.10 (d, J = 9.0 Hz, 1H), 7.94 (t, J = 5.7 Hz, 1H), 7.56 (dd, J = 9.0, 2.1 Hz, 1H), 7.39–7.34 (m, 2H), 7.30 (d, J = 15.6 Hz, 1H), 6.74–6.68 (m, 3H), 6.61 (d, J = 2.5 Hz, 1H), 6.35 (d, J = 15.7 Hz, 1H), 6.29 (d, J = 2.5 Hz, 1H), 3.87 (s, 3H), 3.38–3.33 (m, 2H), 3.28–3.21 (m, 2H), 2.94 (s, 6H), 1.80–1.70 (m, 2H), 1.61 (m, 2H); ^{13}C NMR (100 MHz, DMSO-d_6) δ 165.59, 159.09, 151.00, 144.85, 144.10, 138.86, 138.33, 133.29, 132.83, 129.67, 128.73, 127.94, 127.19, 126.64, 125.51, 122.42, 116.83, 111.97, 96.50, 90.16, 55.11, 42.19, 38.35, 27.05, 25.80; $^m/_z$ (ESI-IT MS, +) 503.67 (M + H$^+$); M$^+$ ($C_{29}H_{31}ClN_4O_2$) requires 502.21; HPLC-DAD: RT, 24.6 min; purity degree (peak relative area), 94.8%.

4.1.2.4. (E)-N-(4-((6-chloro-2-methoxyacridin-4-yl)amino)butyl)-3-(3,4-dimethoxyphenyl)acrylamide (2d). Roasted yellow solid, η = 90%; ^{1}H NMR (400 MHz, DMSO-d_6) δ 8.75 (s, 1H), 8.14 (d, J = 2.0 Hz, 1H), 8.12–8.08 (m, 1H), 8.05 (t, J = 5.7 Hz, 1H), 7.56 (dd, J = 9.0, 2.1 Hz, 1H), 7.35 (d, J = 15.6 Hz, 1H), 7.14 (d, J = 2.0 Hz, 1H), 7.10 (dd, J = 8.3, 2.0 Hz, 1H), 6.99–6.94 (m, 1H), 6.72 (t, J = 5.8 Hz, 1H), 6.62 (d, J = 2.5 Hz, 1H), 6.51 (d, J = 15.7 Hz, 1H), 6.30 (d, J = 2.4 Hz, 1H), 3.87 (s, 3H), 3.78 (d, J = 3.6 Hz, 6H), 3.41–3.31 (m, 2H), 3.26 (q, J = 6.7 Hz, 2H), 1.81–1.69 (m, 2H), 1.68–1.56 (m, 2H); ^{13}C NMR (100 MHz, DMSO-d_6) δ 165.16, 159.09, 150.01, 148.87, 144.85, 144.11, 138.47, 138.33, 133.30, 132.84, 129.69, 127.95, 127.76, 127.19, 126.65, 125.52, 121.26, 120.06, 111.74, 109.94, 96.51, 90.17, 55.52, 55.39, 55.11, 42.18, 38.42, 31.13, 29.81, 26.97, 25.79; $^m/_z$ (ESI-IT MS, +) 520.54 (M + H$^+$); M$^+$ ($C_{29}H_{30}ClN_3O_4$) requires 519.19; HPLC-DAD: RT, 25.0 min; purity degree (peak relative area), 99.5%.

4.1.2.5. (E)-N-(4-((6-chloro-2-methoxyacridin-4-yl)amino)butyl)-3-(4-nitrophenyl)acrylamide (2e). Dark red solid, η = 70%; ^{1}H NMR (400 MHz, DMSO-d_6) δ 8.75 (s, 1H), 8.31 (t, J = 5.7 Hz, 1H), 8.28–8.22 (m, 2H), 8.13 (d, J = 2.2 Hz, 1H), 8.10 (d, J = 9.0 Hz, 1H), 7.84–7.80 (m, 2H), 7.58–7.50 (m, 2H), 6.81 (d, J = 15.8 Hz, 1H), 6.72 (t, J = 5.8 Hz, 1H), 6.61 (d, J = 2.4 Hz, 1H), 6.30 (d, J = 2.5 Hz, 1H), 3.87 (s, 3H), 3.41–3.33 (m, 2H), 3.30–3.25 (m, 2H), 1.82–1.70 (m, 2H), 1.70–1.59 (m, 2H); ^{13}C NMR (100 MHz, DMSO-d_6) δ 164.66, 159.58, 147.93, 145.33, 144.59, 142.10, 138.82, 136.64, 133.79, 133.33, 130.18, 129.00, 128.44, 127.67, 127.10, 126.00, 124.56, 97.02, 90.67, 55.61, 42.64, 39.06, 27.32, 26.25; $^m/_z$ (ESI-IT MS, +) 505.47 (M + H$^+$); M$^+$ ($C_{27}H_{25}ClN_4O_4$) requires 504.16; HPLC-DAD: RT, 26.4 min; purity degree (peak relative area), 97.7%.

4.1.2.6. (E)-N-(4-((6-chloro-2-methoxyacridin-4-yl)amino)butyl)-3-(4-fluorophenyl)acrylamide (2f). Orange solid, η = 92%; ^{1}H NMR (400 MHz, DMSO-d_6) δ 8.75 (s, 1H), 8.18–8.12 (m, 2H), 8.10 (d, J = 9.0 Hz, 1H), 7.65–7.58 (m, 2H), 7.56 (dd, J = 9.0, 2.1 Hz, 1H), 7.41 (d, J = 15.8 Hz, 1H), 7.29–7.19 (m, 2H), 6.72 (t, J = 5.8 Hz, 1H), 6.61 (d, J = 2.5 Hz, 1H), 6.57 (d, J = 15.8 Hz, 1H), 6.30 (d, J = 2.5 Hz, 1H), 3.87 (s, 3H), 3.42–3.34 (m, 2H), 3.29–3.23 (m, 2H), 1.81–1.70 (m, 2H), 1.67–1.59 (m, 2H); ^{13}C NMR (100 MHz, DMSO-d_6) δ 164.79, 159.09, 144.85, 144.11, 138.34, 137.23, 133.31, 132.84, 129.62, 129.54, 127.95, 127.19, 126.65, 125.52, 122.25, 115.96, 115.74, 96.52, 90.19, 55.11, 42.17, 38.46, 31.13, 29.82, 26.92, 25.78; $^m/_z$ (ESI-IT MS, +) 478.93 (M + H$^+$); M$^+$ ($C_{27}H_{25}ClFN_3O_2$) requires 477.16; HPLC-DAD: RT, 26.6 min; purity degree (peak relative area), 98.8%.

4.1.2.7. (E)-N-(4-((6-chloro-2-methoxyacridin-4-yl)amino)butyl)-3-(p-tolyl)acrylamide (2g). Orange solid, η = 98%; ^{1}H NMR (400 MHz, DMSO-d_6) δ 8.75 (s, 1H), 8.16–8.07 (m, 3H), 7.56 (dd, J = 8.9, 2.1 Hz, 1H), 7.47–7.41 (m, 2H), 7.38 (d, J = 15.7 Hz, 1H), 7.24–7.17 (m, 2H), 6.72 (t, J = 5.8 Hz, 1H), 6.61 (d, J = 2.5 Hz, 1H), 6.57 (d, J = 15.8 Hz, 1H), 6.29 (d, J = 2.5 Hz, 1H), 3.87 (s, 3H), 3.40–3.34 (m, 2H), 3.26 (q, J = 6.6 Hz, 2H), 2.31 (s, 2H), 1.80–1.70 (m, 1H), 1.67–1.57 (m, 1H); ^{13}C NMR (100 MHz, DMSO-d_6) δ 164.99, 159.08, 144.84, 144.10, 139.03, 138.35, 138.33, 133.29, 132.83, 132.20, 129.68, 129.48, 127.94, 127.41, 127.19, 126.64, 125.51, 121.29, 96.51, 90.16, 55.10, 42.17, 38.42, 31.13, 29.81, 26.95, 25.78, 20.90; $^{m}/_{z}$ (ESI-IT MS, +) 474.20 (M + H$^+$); M$^+$ ($C_{28}H_{28}ClN_3O_2$) requires 473.19; HPLC-DAD: RT, 27.5 min; purity degree (peak relative area), 96.9%.

4.1.2.8. (E)-3-(4-bromophenyl)-N-(4-((6-chloro-2-methoxyacridin-4-yl)amino)butyl)acrylamide (2h). Brown solid, η = 52%; ^{1}H NMR (400 MHz, DMSO-d_6) δ 8.75 (s, 1H), 8.17 (t, J = 5.7 Hz, 1H), 8.14 (d, J = 2.2 Hz, 1H), 8.10 (d, J = 9.0 Hz, 1H), 7.58–7.62 (m, 2H), 7.56 (dd, J = 8.9, 2.1 Hz, 1H), 7.49–7.52 (m, 2H), 7.39 (d, J = 15.8 Hz, 1H), 6.72 (t, J = 5.8 Hz, 1H), 6.64 (d, J = 15.8 Hz, 1H), 6.62 (d, J = 2.4 Hz, 1H), 6.30 (d, J = 2.5 Hz, 1H), 3.87 (s, 3H), 3.24–3.36 (m, 4H), 1.72–1.79 (m, 2H), 1.59–1.66 (m, 2H); ^{13}C NMR (100 MHz, DMSO-d_6) δ 165.13, 159.58, 145.33, 144.60, 138.82, 137.65, 134.76, 133.79, 133.33, 132.34, 130.18, 129.89, 128.44, 127.68, 127.14, 126.01, 123.70, 122.95, 97.01, 90.66, 55.60, 42.65, 38.97, 27.39, 26.26; $^{m}/_{z}$ (ESI-IT MS, +) 540.64 (M + H$^+$); M$^+$ (C27$H_{25}BrClN_3O_3$) requires 537.08; HPLC-DAD: RT, 28.3 min; purity degree (peak relative area), 99.7%.

4.1.2.9. (E)-N-(4-((6-chloro-2-methoxyacridin-4-yl)amino)butyl)-3-(3-fluorophenyl)acrylamide (2i). Yellow solid, η = 84%; ^{1}H NMR (400 MHz, DMSO-d_6) δ 8.75 (s, 1H), 8.19 (t, J = 5.6 Hz, 1H), 8.14 (d, J = 2.2 Hz, 1H), 8.10 (d, J = 9.0 Hz, 1H), 7.56 (dd, J = 8.9, 2.1 Hz, 1H), 7.37–7.47 (m, 4H), 6.72 (t, J = 5.9 Hz, 1H), 6.67 (d, J = 15.8 Hz, 1H), 6.61 (d, J = 2.5 Hz, 1H), 6.30 (d, J = 2.5 Hz, 1H), 3.87 (s, 3H), 3.35–3.37 (m, 2H), 3.25–3.29 (m, 2H), 1.72–1.79 (m, 2H), 1.60–1.67 (m, 2H); ^{13}C NMR (100 MHz, DMSO-d_6) δ 165.05, 159.58, 145.33, 144.59, 138.82, 137.63, 137.61, 133.79, 133.33, 131.37, 131.29, 130.18, 128.44, 127.68, 127.13, 126.01, 124.40, 124.07, 114.43, 114.22, 97.01, 90.66, 55.60, 42.65, 38.98, 27.38, 26.26; $^{m}/_{z}$ (ESI-IT MS, +) 478.73 (M + H$^+$); M$^+$ ($C_{27}H_{25}ClFN_3O_2$) requires 477.16; HPLC-DAD: RT, 26.8 min; purity degree (peak relative area), 95.1%.

4.1.2.10. (E)-N-(4-((6-chloro-2-methoxyacridin-4-yl)amino)butyl)-3-(4-chlorophenyl)acrylamide (2j). Orange solid, η = 25%; ^{1}H NMR (400 MHz, DMSO-d_6) δ 8.75 (s, 1H), 8.17 (t, J = 5.7 Hz, 1H), 8.13 (d, J = 2.1 Hz, 1H), 8.10 (d, J = 9.0 Hz, 1H), 7.59–7.56 (m, 2H), 7.49–7.44 (m, 2H), 7.40 (d, J = 15.8 Hz, 1H), 6.72 (t, J = 5.9 Hz, 1H), 6.67–6.59 (m, 2H), 6.29 (d, J = 2.4 Hz, 1H), 3.87 (s, 3H), 3.35 (d, J = 6.8 Hz, 2H), 3.32–3.22 (m, 2H), 1.81–1.70 (m, 2H), 1.68–1.58 (m, 2H); ^{13}C NMR (100 MHz, DMSO-d_6) δ 164.65, 159.09, 144.84, 144.10, 138.33, 137.07, 133.94, 133.73, 133.30, 132.84, 129.69, 129.14, 128.92, 127.95, 127.19, 126.64, 125.51, 123.15, 96.52, 90.17, 55.11, 42.16, 38.47, 26.90, 25.77; $^{m}/_{z}$ (ESI-IT MS, +) 494.40 (M + H$^+$); M$^+$ ($C_{27}H_{25}Cl_2N_3O_2$) requires 493.13; HPLC-DAD: RT, 28.0 min; purity degree (peak relative area), 99.5%.

4.1.2.11. (E)-N-(4-((6-chloro-2-methoxyacridin-4-yl)amino)butyl)-3-(4-methoxyphenyl)acrylamide (2k). Roasted yellow solid, η = 28%; ^{1}H NMR (400 MHz, $CDCl_3$) δ 8.39 (s, 1H), 8.13 (d, J = 1.7 Hz, 1H), 7.80 (d, J = 8.9 Hz, 1H), 7.56 (d, J = 15.6 Hz, 1H), 7.44–7.34 (m, 3H), 6.91–6.81 (m, 2H), 6.44 (d, J = 2.4 Hz, 2H), 6.28 (d, J = 2.4 Hz, 1H), 6.21 (d, J = 15.6 Hz, 1H), 5.77 (t, J = 5.2 Hz, 1H), 3.91 (s, 3H), 3.81 (s, 3H), 3.47 (q, J = 6.7 Hz, 2H), 3.41–3.32 (m, 2H), 1.93–1.84 (m, 2H), 1.84–1.71 (m, 2H); ^{13}C NMR (100 MHz, $CDCl_3$) δ 166.44, 160.96, 159.51, 145.28, 145.11, 140.69, 139.05, 133.93, 133.06, 129.43, 128.76, 128.23, 128.13, 127.71, 127.13, 125.96, 118.45, 114.33, 97.31, 90.50, 55.46, 55.39, 43.11, 39.60, 27.70, 26.57; $^{m}/_{z}$ (ESI-IT MS, +) 490.80 (M + H$^+$); M$^+$ ($C_{28}H_{28}ClN_3O_3$) requires 489.18; HPLC-DAD: RT, 26.2 min; purity degree (peak relative area), 99.8%.

4.1.2.12. N-(4-((6-chloro-2-methoxyacridin-4-yl)amino)butyl)-cinnamamide (2l). Orange solid, η = 35%; ^{1}H NMR (400 MHz, $CDCl_3$) δ 8.37 (s, 1H), 8.12 (d, J = 1.8 Hz, 1H), 7.78 (d, J = 8.9 Hz, 1H), 7.61 (d, J = 15.6 Hz, 1H), 7.47–7.41 (m, 2H), 7.39 (dd, J = 8.9, 2.0 Hz, 1H), 7.34–7.29 (m, 2H), 6.42 (d, J = 2.4 Hz, 1H), 6.35 (d, J = 15.6 Hz, 1H), 6.27 (d, J = 2.4 Hz, 1H), 5.92 (t, J = 5.3 Hz, 1H), 3.91 (s, 3H), 3.47 (q, J = 6.7 Hz, 2H), 3.35 (t, J = 6.7 Hz, 2H), 1.91–1.83 (m, 2H), 1.81–1.73 (m, 2H); ^{13}C NMR (100 MHz, $CDCl_3$) δ 166.13, 159.47, 145.23, 145.06, 141.03, 138.98, 134.98, 133.94, 133.06, 129.70, 128.88, 128.74, 128.19, 128.06, 127.87, 127.11, 125.92, 120.85, 97.32, 90.50, 55.37, 43.07, 39.64, 27.61, 26.55; $^{m}/_{z}$ (ESI-IT MS, +) 460.67 (M + H$^+$); M$^+$ ($C_{27}H_{26}ClN_3O_2$) requires 459.17; HPLC-DAD: RT, 26.4 min; purity degree (peak relative area), 99.6%.

4.2. In vitro assays

4.2.1. Hepatic stage activity

The *in vitro* inhibition of hepatic infection by the test compounds was determined by measuring the luminescence intensity in lysates of Huh7 cells infected with a firefly luciferase-expressing *P. berghei* line, *PbGFP*-Luccon, as previously described [50]. Huh7 cells were cultured in Roswell Park Memorial Institute 1640 medium (RPMI) supplemented with 10% v/v fetal calf serum, 1% v/v penicillin/streptomycin, 1% v/v nonessential amino acids, 1% v/v glutamine, and 10 mM 4-(2-hydroxyethyl)-1-piperazine ethanesulfonic acid (HEPES), pH 7, and maintained at 37 °C with 5% CO_2. For infection assays, Huh7 cells were seeded in 96-well plates the day before drug treatment and infection. Approximately 1 h prior to infection with sporozoites freshly obtained through disruption of salivary glands of infected female *Anopheles stephensi* mosquitoes, the culture medium in the wells was replaced by infection medium (culture medium supplemented with 50 μg/mL gentamicin and 0.8 μg/mL amphotericin B) containing the appropriate concentration of each compound. In control cells, culture medium was replaced by medium containing the same percentage of DMSO used in compound solutions (0.01%), which is not cytotoxic. After 48 h of infection, inhibition of infection was measured and the effect of the compounds on the viability of Huh7 cells was assessed by the AlamarBlue assay (Invitrogen, UK) using the manufacturer's protocol. Nonlinear regression analysis was employed to fit the normalized results of the dose-response curves, and IC_{50} values were determined using GraphPad Prism 8.0 (GraphPad software, La Jolla, CA, USA). Cytotoxicity was extrapolated from the cell confluency data. All data was then normalized to the DMSO control. Therefore, a decrease in cell confluency, as compared to the DMSO control, was indicative of cytotoxicity.

4.2.2. Gametocytocidal activity

P. falciparum parasites of the high-gametocyte productive NF54-gexp02-Tom line [51] (kindly provided by Prof. Alfred Cortés), which has a genome-integrated tandem Tomato (tdTomato) fluorescent marker gene controlled by an early gametocyte promoter, were used. Parasites were grown in group B human erythrocytes at 3% hematocrit in RPMI-based standard medium supplemented with 10% human plasma and 2 mM choline chloride, and incubated at 37 °C under hypoxia (5% O_2, 5% CO_2, and 90% N_2 at 37 °C). To induce sexual conversion, choline was removed from the medium, in combination with synchronization by sorbitol lysis. Induced cultures were then maintained without choline until the end of the experiment. The effect on gametocyte development was assessed in two independent replicas by adding growing concentrations (0.0048–100 μM) of each compound to the culture. The appearance of stage V gametocytes was daily monitored by light

microscopy. Fifteen days after choline removal, ~80% of gametocytes reached stages IV and V (mature forms). After this time, Giemsa-stained blood smears were prepared and at least 10,000 cells were counted for each condition. A negative control culture without drugs and a positive control treated with the IC_{90} of chloroquine and primaquine, where no gametocytes were observed at the end of the experiment, were also included. Growth inhibition data was transformed through sigmoidal fitting and used to determine the compounds' concentrations required for the reduction of *P. falciparum* viability by 50% (IC_{50}), using the GrapPhad Prism 9 software.

4.2.3. Blood stage activity

Asexual stages of the *P. falciparum* 3D7 strain were grown in group B human erythrocytes at 3% hematocrit using RPMI supplemented with 0.5% (w/v) Albumax II (Life Technologies, New Zealand) and 2 mM L-glutamine. Throughout the whole experiment, parasites were maintained in standard culturing conditions (37 °C, 5% O_2, 5% CO_2, and 90% N_2). Before starting the blood stage activity assays, parasites were synchronized in the ring stage with a 5% sorbitol lysis as described in Ref. [52]. Afterwards, growing concentrations of the different 4-(N-cinnamoylbutyl)aminoacridines (0.0000256–10 μM) were incubated with the parasite culture during 48 h. Finally, cultures were diluted to ca. 1 to 10×10^6 cells/mL and incubated with Syto11 to stain the nuclei. Parasitemia was analyzed by flow cytometry using a LSRFortessa flow cytometer (BD Biosciences, USA) set up with the 4 lasers, 20 parameters standard configuration. The single-cell population was selected on a forward-side scattergram. Syto 11 fluorescence signal was detected by exciting samples at 488 nm and collecting the emission with a 530/30-nm bandpass filter. Growth inhibition was calculated taking as reference values the growth rates of an untreated culture (0% inhibition) and of a chloroquine-treated culture (100% inhibition). Growth inhibition data was transformed through sigmoidal fitting and used to determine the compounds' concentrations required for the reduction of *P. falciparum* viability by 50% (IC_{50}) using the GraphPad Prism 9 software.

4.2.4. Hemolytic activity

Human blood samples were first centrifuged (Centurion scientific Ltd centrifuge with a BRK1001 rotor) at 2500 rpm for 5 min at 4 °C to remove the plasma. The red blood cells (RBC) thus collected were then washed three times with 0.01 M phosphate-buffered saline, pH 7.4 (PBS, Sigma-Aldrich) and diluted to a final 6% hematocrit in PBS. In a 96-well plate, 100 μL of RBCs at 6% hematocrit were plated in the presence of 100 μL of a solution of each compound at 40 μM in 1% DMSO in PBS, and next incubated at 37 °C for 1 h. 1% Triton X-100 in PBS and 1% DMSO in PBS were used as positive and negative controls, respectively. After the 1-h incubation period, the plates were centrifuged (Sigma® 3–30K centrifuge from Sigma Centrifuges GmbH with a swing-out 11222 rotor) at 860×*g* (2500 rpm), for 10 min at 25 °C. Finally, 80 μL of the supernatants were transferred to a new 96-well plate and absorbance (A) at 450 nm was measured in a microplate reader (Multiskan GO, Thermo Scientific). The percentage of hemolysis was calculated for each test compound using the following equation:

$$Hemolysis = \frac{A\ (peptide) - A\ (negative\ control)}{A\ (positive\ control) - A\ (negative\ control)}$$

Ethics statement

The human blood used in this work was obtained from Centro Hospitalar Universitário do Porto (CHUP) under a collaboration protocol with our group. Prior to being delivered to us, the blood units collected go through analytical checks specified in the current legislation. Each unit data was anonymized and permanently dissociated to ensure the non-identification of the blood donor, and only an identification label with the gender and type of blood was attached to the samples. The blood samples have been used only for the research purpose herein described.

Funding

This work received financial support from PT national funds (FCT/MCTES, Fundação para a Ciência e Tecnologia and Ministério da Ciência, Tecnologia e Ensino Superior) through the project CIRCNA/BRB/0281/2019.

Declaration of competing interest

The authors declare that they have no known competing financial interests or personal relationships that could have appeared to influence the work reported in this paper.

Data availability

Data will be made available on request.

Acknowledgment

The authors further thank FCT/MCTES for supporting Research Units LAQV-REQUIMTE (UIDB/50006/2020) and for the Doctoral Grant to MF (SRFH/BD/147354/2019). MP further acknowledges the "la Caixa" Foundation for Grant HR21-848. ISGlobal and IBEC are members of the CERCA Programme, Generalitat de Catalunya. We acknowledge support from the Ministerio de Ciencia e Innovación/Agencia Estatal de Investigación (MCIN/AEI/ 10.13039/501100011033) through the "Centro de Excelencia Severo Ochoa 2019-2023" Program (CEX2018-000806-S). This research is part of ISGlobal's Program on the Molecular Mechanisms of Malaria which is partially supported by the Fundación Ramón Areces.

Appendix A. Supplementary data

Supplementary data to this article can be found online at https://doi.org/10.1016/j.ejmech.2023.115575.

Abbreviations

ACT	artemisinin-based combination therapies
CQ	chloroquine
DIEA	*N,N*-diisopropylethylamine
ESI-IT MS	electrospray ionization-ion trap mass spectrometry
HEPES	4-(2-hydroxyethyl)-1-piperazine ethanesulfonic acid
P	*Plasmodium*
PQ	primaquine
QN	quinacrine
RPMI	roswell Park Memorial Institute 1640 medium
RT	retention time
SAR	structure and activity relationship
SD	standard deviation
TBTU	O-(Benzotriazol-1-yl)-N,N,N′,N′-tetramethyluronium tetrafluoroborate
TQ	Tafenoquine

References

[1] World Health Organization, World Malaria Report, 2022.
[2] D. Menard, A. Dondorp, Antimalarial drug resistance: a threat to malaria elimination, Cold Spring Harb. Perspect Med. 7 (2017).
[3] World Health Organization, Artemisinin Resistance and Artemisinin-Based Combination Therapy Efficacy, 2018.
[4] C. Nsanzabana, Resistance to artemisinin combination therapies (ACTs): do not forget the partner drug, Trav. Med. Infect. Dis. 4 (2019) 26.
[5] P.J. Rosenthal, Has artemisinin resistance emerged in Africa? Lancet Infect. Dis. 21 (2021) 1056–1057.

[6] N. Noreen, A. Ullah, S.M. Salman, Y. Mabkhot, A. Alsayari, S.L. Badshah, New insights into the spread of resistance to artemisinin and its analogues, J. Glob. Antimicrobial Resist. 27 (2021) 142–149.
[7] B. Balikagala, N. Fukuda, M. Ikeda, O.T. Katuro, S.-I. Tachibana, M. Yamauchi, W. Opio, S. Emoto, D.A. Anywar, E. Kimura, N.M.Q. Palacpac, E.I. Odongo-Aginya, M. Ogwang, T. Horii, T. Mita, Evidence of artemisinin-resistant malaria in Africa, N. Engl. J. Med. 385 (2021) 1163–1171.
[8] N.S. Tibon, C.H. Ng, S.L. Cheong, Current progress in antimalarial pharmacotherapy and multi-target drug discovery, Eur. J. Med. Chem. 188 (2020), 111983.
[9] V. Parvathaneni, N.S. Kulkarni, A. Muth, V. Gupta, Drug repurposing: a promising tool to accelerate the drug discovery process, Drug Discov. Today 24 (2019) 2076–2085.
[10] C. Teixeira, N. Vale, B. Pérez, A. Gomes, J.R.B. Gomes, P. Gomes, "Recycling" classical drugs for malaria, Chem. Rev. 114 (2014) 11164–11220.
[11] M.J. Araújo, J. Bom, R. Capela, C. Casimiro, P. Chambel, P. Gomes, J. Iley, F. Lopes, J. Morais, R. Moreira, E. de Oliveira, V. do Rosário, N. Vale, Imidazolidin-4-one derivatives of primaquine as novel transmission-blocking antimalarials, J. Med. Chem. 48 (2005) 888–892.
[12] N. Vale, F. Nogueira, V.E. do Rosário, P. Gomes, R. Moreira, Primaquine dipeptide derivatives bearing an imidazolidin-4-one moiety at the N-terminus as potential antimalarial prodrugs, Eur. J. Med. Chem. 44 (2009) 2506–2516.
[13] N. Vale, M. Prudêncio, C.A. Marques, M.S. Collins, J. Gut, F. Nogueira, J. Matos, P. J. Rosenthal, M.T. Cushion, V.E. do Rosário, M.M. Mota, R. Moreira, P. Gomes, Imidazoquines as antimalarial and antipneumocystis agents, J. Med. Chem. 52 (2009) 7800–7807.
[14] J. Matos, F.P.d. Cruz, É. Cabrita, J. Gut, F. Nogueira, V.E.d. Rosário, R. Moreira, P. J. Rosenthal, M. Prudêncio, P. Gomes, Novel potent metallocenes against liver stage malaria, Antimicrob. Agents Chemother. 56 (2012) 1564–1570.
[15] B.C. Pérez, C. Teixeira, I.S. Albuquerque, J. Gut, P.J. Rosenthal, J.R.B. Gomes, M. Prudêncio, P. Gomes, N-cinnamoylated chloroquine analogues as dual-stage antimalarial leads, J. Med. Chem. 56 (2013) 556–567.
[16] A. Gomes, B. Pérez, I. Albuquerque, M. Machado, M. Prudêncio, F. Nogueira, C. Teixeira, P. Gomes, N-cinnamoylation of antimalarial classics: quinacrine analogues with decreased toxicity and dual-stage activity, ChemMedChem 9 (2014) 305–310.
[17] M. Fonte, N. Fagundes, A. Gomes, R. Ferraz, C. Prudêncio, M.J. Araújo, P. Gomes, C. Teixeira, Development of a synthetic route towards N4,N9-disubstituted 4,9-diaminoacridines: on the way to multi-stage antimalarials, Tetrahedron Lett. 60 (2019) 1166–1169.
[18] M. Fonte, N. Tassi, D. Fontinha, I. Bouzón-Arnáiz, R. Ferraz, M.J. Araújo, X. Fernàndez-Busquets, M. Prudêncio, P. Gomes, C. Teixeira, 4,9-Diaminoacridines and 4-aminoacridines as dual-stage antiplasmodial hits, ChemMedChem 16 (2021) 788–792.
[19] M. Fonte, N. Tassi, P. Gomes, C. Teixeira, Acridine-based antimalarials—from the very first synthetic antimalarial to recent developments, Molecules 26 (2021) 600.
[20] C. Rasmussen, P. Alonso, P. Ringwald, Current and emerging strategies to combat antimalarial resistance, Expert Rev. Anti-infect. Ther. 20 (2022) 353–372.
[21] N. Vale, R. Moreira, P. Gomes, Primaquine revisited six decades after its discovery, Eur. J. Med. Chem. 44 (2009) 937–953.
[22] T. Rodrigues, M. Prudêncio, R. Moreira, M.M. Mota, F. Lopes, Targeting the liver stage of malaria parasites: a yet unmet goal, J. Med. Chem. 55 (2012) 995–1012.
[23] E.A. Ashley, J. Recht, N.J. White, Primaquine: the risks and the benefits, Malar. J. 13 (2014) 418.
[24] A. Mayence, J.J. Vanden Eynde, A. Tafenoquine, Novel FDA-approved prodrug for the radical cure of Plasmodium vivax malaria and prophylaxis of malaria, Pharmaceuticals 12 (2019) (2018) 115.
[25] A. Talevi, Multi-target pharmacology: possibilities and limitations of the "skeleton key approach" from a medicinal chemist perspective, Front. Pharmacol. 6 (2015).
[26] X.H. Makhoba, C. Viegas Jr., R.A. Mosa, F.P.D. Viegas, O.J. Pooe, Potential impact of the multi-target drug approach in the treatment of some complex diseases, Drug Des. Dev. Ther. 14 (2020) 3235–3249.
[27] B. Meunier, Towards antimalarial hybrid drugs, in: Polypharmacology in Drug Discovery, 2012, pp. 423–439.
[28] B. Meunier, Hybrid molecules with a dual mode of action: dream or reality? Acc. Chem. Res. 41 (2008) 69–77.
[29] Y. Li, A. Loureiro, M. Nguyen, M. Laurent, C. Bijani, F. Benoit-Vical, A. Robert, Y. Liu, B. Meunier, Synthesis and antimalarial activities of new hybrid atokel molecules, ChemistryOpen 11 (2022), e202200064.
[30] M. Ouji, G. Barnoin, Á. Fernández Álvarez, J.-M. Augereau, C. Hemmert, F. Benoit-Vical, H. Gornitzka, Hybrid gold(I) NHC-artemether complexes to target falciparum malaria parasites, Molecules 25 (2020) 2817.
[31] M.M. Santos, R. Moreira, Michael acceptors as cysteine protease inhibitors, Mini Rev. Med. Chem. 7 (2007) 1040–1050.
[32] B.R. Shenai, B.J. Lee, A. Alvarez-Hernandez, P.Y. Chong, C.D. Emal, R.J. Neitz, W. R. Roush, P.J. Rosenthal, Structure-activity relationships for inhibition of cysteine protease activity and development of Plasmodium falciparum by peptidyl vinyl sulfones, Antimicrob. Agents Chemother. 47 (2003) 154–160.
[33] I.D. Kerr, J.H. Lee, C.J. Farady, R. Marion, M. Rickert, M. Sajid, K.C. Pandey, C. R. Caffrey, J. Legac, E. Hansell, J.H. McKerrow, C.S. Craik, P.J. Rosenthal, L. S. Brinen, Vinyl sulfones as antiparasitic agents and a structural basis for drug design, J. Biol. Chem. 284 (2009) 25697–25703.
[34] P.J. Rosenthal, J.E. Olson, G.K. Lee, J.T. Palmer, J.L. Klaus, D. Rasnick, Antimalarial effects of vinyl sulfone cysteine proteinase inhibitors, Antimicrob. Agents Chemother. 40 (1996) 1600–1603.
[35] P.M.C. Glória, J. Gut, L.M. Gonçalves, P.J. Rosenthal, R. Moreira, M.M.M. Santos, Aza vinyl sulfones: synthesis and evaluation as antiplasmodial agents, Bioorg. Med. Chem. 19 (2011) 7635–7642.
[36] S. Previti, R. Ettari, S. Cosconati, G. Amendola, K. Chouchene, A. Wagner, U. A. Hellmich, K. Ulrich, R.L. Krauth-Siegel, P.R. Wich, I. Schmid, T. Schirmeister, J. Gut, P.J. Rosenthal, S. Grasso, M. Zappalà, Development of novel peptide-based Michael acceptors targeting rhodesain and falcipain-2 for the treatment of neglected tropical diseases (NTDs), J. Med. Chem. 60 (2017) 6911–6923.
[37] J. Kanaani, H. Ginsburg, Effects of cinnamic acid derivatives on in vitro growth of Plasmodium falciparum and on the permeability of the membrane of malaria-infected erythrocytes, Antimicrob. Agents Chemother. 36 (1992) 1102–1108.
[38] B.-B. F, V.-B. C, M. B, Prithwiraj De, Cinnamic acid derivatives in tuberculosis, malaria and cardiovascular diseases - a review, Curr. Org. Chem. 16 (2012) 747–768.
[39] A.T. Silva, C.M. Bento, A.C. Pena, L.M. Figueiredo, C. Prudêncio, L. Aguiar, T. Silva, R. Ferraz, M.S. Gomes, C. Teixeira, P. Gomes, Cinnamic acid conjugates in the rescuing and repurposing of classical antimalarial drugs, Molecules 25 (2020) 66.
[40] J. Wiesner, A. Mitsch, P. Wißner, H. Jomaa, M. Schlitzer, Structure–activity relationships of novel anti-malarial agents. Part 2: cinnamic acid derivatives, Bioorg. Med. Chem. Lett 11 (2001) 423–424.
[41] B. Pérez, C. Teixeira, A.S. Gomes, I.S. Albuquerque, J. Gut, P.J. Rosenthal, M. Prudêncio, P. Gomes, In vitro efficiency of 9-(N-cinnamoylbutyl)aminoacridines against blood- and liver-stage malaria parasites, Bioorg. Med. Chem. Lett 23 (2013) 610–613.
[42] B. Pérez, C. Teixeira, J. Gut, P.J. Rosenthal, J.R.B. Gomes, P. Gomes, Cinnamic acid/chloroquinoline conjugates as potent agents against chloroquine-resistant Plasmodium falciparum, ChemMedChem 7 (2012) 1537–1540.
[43] N. Ruwizhi, B.A. Aderibigbe, Cinnamic acid derivatives and their biological efficacy, Int. J. Mol. Sci. 21 (2020) 5712.
[44] M. Prudêncio, A. Rodriguez, M.M. Mota, The silent path to thousands of merozoites: the Plasmodium liver stage, Nat. Rev. Microbiol. 4 (2006) 849–856.
[45] Â.F. Chora, M.M. Mota, M. Prudêncio, The reciprocal influence of the liver and blood stages of the malaria parasite's life cycle, Int. J. Parasitol. 52 (2022) 711–715.
[46] K. Van Dyke, C. Lantz, C. Szustkiewicz, Quinacrine: mechanisms of antimalarial action, Science 169 (1970) 492–493.
[47] R. Ehsanian, C. Van Waes, S.M. Feller, Beyond DNA binding - a review of the potential mechanisms mediating quinacrine's therapeutic activities in parasitic infections, inflammation, and cancers, Cell Commun. Signal. 9 (2011) 13.
[48] A. Gomes, I. Fernandes, C. Teixeira, N. Mateus, M.J. Sottomayor, P. Gomes, A quinacrine analogue selective against gastric cancer cells: insight from biochemical and biophysical studies, ChemMedChem 11 (2016) 2703–2712.
[49] C. Upadhyay, M. Chaudhary, R.N. De Oliveira, A. Borbas, P. Kempaiah, P. S, B. Rathi, Fluorinated scaffolds for antimalarial drug discovery, Expet Opin. Drug Discov. 15 (2020) 705–718.
[50] I.H.J. Ploemen, M. Prudêncio, B.G. Douradinha, J. Ramesar, J. Fonager, G.-J. van Gemert, A.J.F. Luty, C.C. Hermsen, R.W. Sauerwein, F.G. Baptista, M.M. Mota, A. P. Waters, I. Que, C.W.G.M. Lowik, S.M. Khan, C.J. Janse, B.M.D. Franke-Fayard, Visualisation and quantitative analysis of the rodent malaria liver stage by real time imaging, PLoS One 4 (2009), e7881.
[51] H.P. Portugaliza, O. Llorà-Batlle, A. Rosanas-Urgell, A. Cortés, Reporter lines based on the gexp02 promoter enable early quantification of sexual conversion rates in the malaria parasite Plasmodium falciparum, Sci. Rep. 9 (2019), 14595.
[52] C. Lambros, J.P. Vanderberg, Synchronization of Plasmodium falciparum erythrocytic stages in culture, J. Parasitol. 65 (1979) 418–420.